STEM CELLS TRANSLATIONAL MEDICINE®

CELL-BASED DRUG DEVELOPMENT, SCREENING, AND TOXICOLOGY

Stem Cell-Derived Immature Human Dorsal Root Ganglia Neurons to Identify Peripheral Neurotoxicants

LISA HOELTING,[a,b] STEFANIE KLIMA,[a] CHRISTIAAN KARREMAN,[a] MARIANNA GRINBERG,[c] JOHANNES MEISIG,[d,e] MARGIT HENRY,[f] TAMARA ROTSHTEYN,[f] JÖRG RAHNENFÜHRER,[c] NILS BLÜTHGEN,[d,e] AGAPIOS SACHINIDIS,[f] TANJA WALDMANN,[a] MARCEL LEIST[a]

Key Words. Human pluripotent stem cells • Neural differentiation • Peripheral neuropathies • In vitro drug and toxicity testing

ABSTRACT

Safety sciences and the identification of chemical hazards have been seen as one of the most immediate practical applications of human pluripotent stem cell technology. Protocols for the generation of many desirable human cell types have been developed, but optimization of neuronal models for toxicological use has been astonishingly slow, and the wide, clinically important field of peripheral neurotoxicity is still largely unexplored. A two-step protocol to generate large lots of identical peripheral human neuronal precursors was characterized and adapted to the measurement of peripheral neurotoxicity. High content imaging allowed an unbiased assessment of cell morphology and viability. The computational quantification of neurite growth as a functional parameter highly sensitive to disturbances by toxicants was used as an endpoint reflecting specific neurotoxicity. The differentiation of cells toward dorsal root ganglia neurons was tracked in relation to a large background data set based on gene expression microarrays. On this basis, a peripheral neurotoxicity (PeriTox) test was developed as a first toxicological assay that harnesses the potential of human pluripotent stem cells to generate cell types/tissues that are not otherwise available for the prediction of human systemic organ toxicity. Testing of more than 30 chemicals showed that human neurotoxicants and neurite growth enhancers were correctly identified. Various classes of chemotherapeutic agents causing human peripheral neuropathies were identified, and they were missed when tested on human central neurons. The PeriTox test we established shows the potential of human stem cells for clinically relevant safety testing of drugs in use and of new emerging candidates. STEM CELLS TRANSLATIONAL MEDICINE *2016;5:476–487*

SIGNIFICANCE

The generation of human cells from pluripotent stem cells has aroused great hopes in biomedical research and safety sciences. Neurotoxicity testing is a particularly important application for stem cell-derived somatic cells, as human neurons are hardly available otherwise. Also, peripheral neurotoxicity has become of major concern in drug development for chemotherapy. The first neurotoxicity test method was established based on human pluripotent stem cell-derived peripheral neurons. The strategies exemplified in the present study of reproducible cell generation, cell function-based test system establishment, and assay validation provide the basis for a drug safety assessment on cells not available otherwise.

[a]Doerenkamp-Zbinden Lab for In Vitro Toxicology and Biomedicine and [b]Konstanz Graduate School Chemical Biology KORS-CB, University of Konstanz, Konstanz, Germany; [c]Faculty of Statistics, TU Dortmund University, Dortmund, Germany; [d]Institute of Pathology, Charité-Universitätsmedizin, Berlin, Germany; [e]Integrative Research Institute for the Life Sciences and Institute for Theoretical Biology, Humboldt Universität, Berlin, Germany; [f]Institute of Neurophysiology and Center for Molecular Medicine Cologne, University of Cologne, Cologne, Germany

Correspondence: Lisa Hoelting, M.Sc., University of Konstanz, Box M657, Konstanz D-78457, Germany. Telephone: 49-7531-88-5331; E-Mail: Lisa.Hoelting@uni-konstanz.de

Received May 19, 2015; accepted for publication November 19, 2015; published Online First on March 1, 2016.

1066-5099/2016/$20.00/0

http://dx.doi.org/10.5966/sctm.2015-0108

INTRODUCTION

Peripheral neurotoxicity is a major issue in drug development and environmental medicine. For instance, chemical-induced axonopathies play an important role in the toxicity of drugs and environmental chemicals [1, 2], and testing systems for this pathological endpoint are in high demand. Moreover, the growth of neurites during development has been considered a key biological process that can be targeted by chemicals [3]. Therefore, the testing of neurotoxicity on the basis of human cells is an emerging research field in safety sciences. The generation of the relevant target cell populations from human pluripotent stem cells has aroused great hopes in biomedical research and the safety sciences [4–6] that model systems will be established to identify neurotoxicity hazards and to devise countermeasures.

The currently used methods to test for neurotoxicity are all based on experimental animals in accordance with Organization

Economic Co-operation and Development test guideline 424. These tests cover all relevant target cell types but are expensive, labor-intensive, and associated with uncertainties in the extrapolation of the results to humans [5, 7, 8]. Therefore, the U.S. National Research Council and major regulatory agencies have recommended new strategies for toxicity testing (Tox21) based on in vitro high throughput testing and cell-based systems, ideally of human origin [9, 10]. Thus, in vitro neurotoxicity and developmental neurotoxicity assays are required that can ultimately be assembled into a test battery covering all relevant cell types and endpoints [8].

The first newer approaches to establish test systems for neurite integrity and growth used rodent primary neural cultures and immortalized human and nonhuman clonal cell lines to measure neurite length or to quantify the number of neurites and dendrites in low-density cultures [11–13]. The effect of chemicals on neurite network formation and function has also been assessed by manual counting of neurite interconnections [14] or by recording spontaneous network activity [15]. More recently, more physiological high-density cultures have been used for quantification of neurite growth and viability by automated high-content image analysis, which enables a better separation between specific neurite toxicity and general cytotoxicity [16, 17]. Human neurons have also been generated from pluripotent stem cells (PSCs) for neurite toxicity testing. This approach showed the potential of the use of stem cells to generate target cell types not otherwise accessible [18]. However, most work has focused on mechanistic case studies, and broad applications for unbiased comparisons across many compound classes have been extremely sparse. Moreover, it has proved surprisingly difficult to generate a system that distinguishes neurotoxicity from general cytotoxicity, that allows sufficient throughput for realistic application (most published studies have reported on only ≤ 3 specific neurotoxicants), and that is technically robust enough, concerning cell differentiation and its toxicological readout.

The protein expression patterns in neurites of different neuronal types (e.g., peripheral/central or human/mouse) can differ, and this will also affect the abundance of modulators of axonal degeneration [19–21]. Therefore, it appears advisable to choose a toxicological model system that matches its pathological reference system (e.g., human peripheral axons) as closely as possible, as far as the type of neurons and the species of their origin are concerned.

As primary human peripheral cells are hardly available, we used human stem cells to generate immature dorsal root ganglia neuron (iDRG) cells for use in neurite toxicity testing. Previous experience in the field has shown that it is challenging to measure neurite toxicity independent from that of general cytotoxicity [14, 22, 23]. Such specificity can be obtained if a model system depends on a functional feature that is only found in neurites (e.g., outgrowth). Growing neurites have been reported to be more susceptible to some neurite-damaging toxicants than established neurites. Therefore, cell culture systems with strong neurite growth will allow the detection of toxicant effects at concentrations that did not compromise cell survival [14, 16]. To establish a new method to assess peripheral neurotoxicity, we therefore used iDRG cells and followed their neurite growth. To test for cell-type specific effects, we compared a broad range of compounds in this new peripheral neurotoxicity (PeriTox) test with the Lund human mesencephalic cells (LUHMES) neurite test (using central neurons), and clearly different hit patterns were revealed.

Materials and Methods

Cell Culture and Neural Differentiation

Human pluripotent stem cell lines were cultured according to standard protocols [24] and differentiated into immature dorsal root ganglia neurons, as described previously [25], with modifications as shown in Figure 1. In detail, the H9 human embryonic stem cell (hESC) line (WA09 line) was obtained from WiCell Research Institute (Madison, WI, http://www.wicell.org) and minicircle induced pluripotent stem cell (mc-iPSC) from System Biosciences (model no. SC301A-1; System Biosciences, Mountain View, CA, http://www.systembio.com). The import of cells and experiments were authorized under license no. 170-79-1-4-27 (Robert Koch Institute, Berlin, Germany, http://www.rki.de). Differentiation of the pluripotent stem cell lines hESC-H9 and mc-iPSC to iDRG cells was prepared on the day of differentiation minus 3 (DoD−3′) by replating human pluripotent stem cells (hPSCs) in a single cell suspension onto Matrigel-coated plates (BD Biosciences, Franklin Lakes, NJ, http://www.bdbiosciences.com; 30,000 cells per cm^2) in "conditioned" keratinocyte culture medium (KCM). This KCM was conditioned for 24 hours on mitomycin C-inactivated mouse embryonic fibroblasts. It was freshly supplemented with 10 ng/ml fibroblast growth factor 2 (R&D Systems, Minneapolis, MN, http://www.rndsystems.com) and ROCK inhibitor Y-27632 (10 μM; Tocris Bioscience, Bristol, U.K., http://www.tocris.com). On DoD0′, neural differentiation was started by adding neural differentiation medium KSR-S (knockout Dulbecco's modified Eagle's medium [DMEM] with 15% serum replacement, 1 $\times$ Glutamax, 1 $\times$ nonessential amino acids, and 50 μM β-mercaptoethanol; all ingredients from Invitrogen, Darmstadt, Germany, http://www.thermofisher.com) and the combination of six small molecule pathway inhibitors. In detail, noggin (35 ng/ml; R&D Systems), dorsomorphin (600 nM; Tocris Bioscience), and SB-431642 (10 μM; Tocris Bioscience) were added on DoD0′–5′ and CHIR99021 (1.5 μM; Axon Medchem, Vienna, VA, http://www/axonmedchem.com), SU5402 (1.5 μM; Tocris Bioscience), and DAPT (γ-Secretase Inhibitor IX; 5 μM; Merck, Darmstadt, Germany, http://www.merck.de) were added on DoD2′–8′. From DoD4′ onward, the medium was gradually replaced by N2-S medium (DMEM/F12, with 2 mM Glutamax, 0.1 mg/ml apotransferrin, 1.55 mg/ml glucose, 25 μg/ml insulin, 100 μM putrescine, 30 nM selenium, and 20 nM progesterone). On DoD8′, the cells were cryopreserved. After thawing, the obtained neuronal precursors were cultured in 25% KSR-S and 75% N2-S medium supplemented with CHIR99021 (1.5 μM), SU5402 (1.5 μM), and DAPT (5 μM) and seeded at a density of 0.1×10^6 cells per milliliter onto Matrigel-coated wells (BD Biosciences). For further differentiation, one half of the medium was changed on DoD1 and again on DoD2. From DoD3 onward, the cells were grown in the presence of brain-derived neurotrophic factor, glia-derived neurotrophic factor, and nerve growth factor (25 ng/ml; R&D Systems) to facilitate further differentiation and maturation into peripheral neurons.

Transcriptome Analysis

RNA was extracted at the indicated DoD (hESCs, DoD8′, DoD1, DoD4, DoD7) from four independent differentiations and

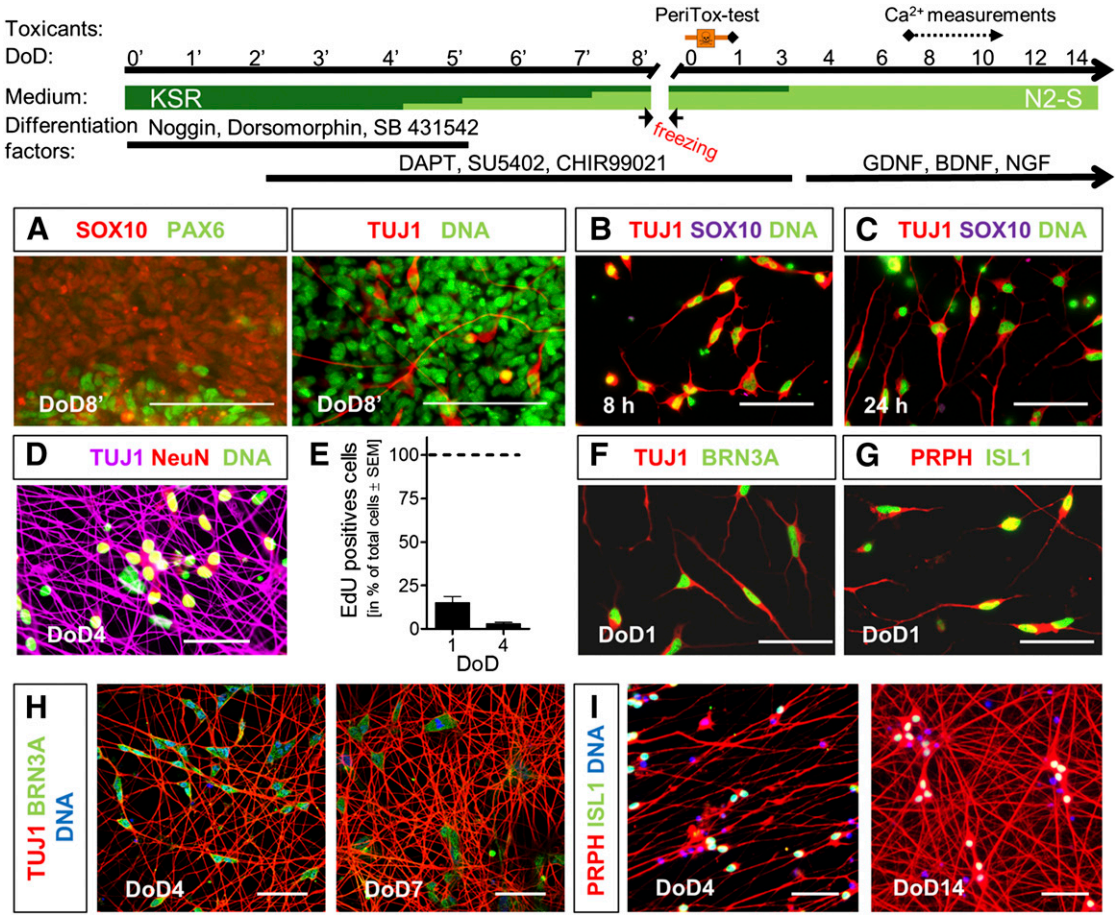

Figure 1. Generation of human immature dorsal root ganglia neuron (iDRG) cells for toxicity testing. Pluripotent stem cells were differentiated in a two-step procedure, as indicated. **(A–D):** Immunocytochemical characterization of hESC-derived cells. Labels are color keyed to images. **(E):** Proliferating cells (EdU^+) were quantified (mean ± SEM; $n = 3$). **(F–I):** Immunocytochemical characterization of iDRG cells after thawing. Labels are color keyed to images. Scale bars = 100 μm **(A)** and 50 μm **(B–D, F–I)**. Abbreviations: BDNF, brain-derived neurotrophic factor; DoD, day of differentiation; GDNF, glia-derived neurotrophic factor; hESC, human embryonic stem cell; NGF, nerve growth factor.

prepared for microarray hybridization on Affymetrix Human Genome U133 plus 2.0 (Affymetrix, Santa Clara, CA, http://www.affymetrix.com), as described previously [26, 27]. Data analysis was performed as described in supplemental online data.

Immunocytochemistry

At the indicated DoD, the cells were fixed in 4% paraformaldehyde/2% sucrose before permeabilization in 0.5% Triton X-100. After blocking in 5% bovine serum albumin/phosphate-buffered saline for 1 hour, the cells were incubated with primary antibodies for 1 hour at room temperature and stained with the appropriate secondary antibody for 30 minutes. DNA was stained with H-33342 (1 μg/ml), and coverslips were mounted in FluorSave reagent (Merck Millipore, Billerica, MA, http://www.merckmillipore.com).

Peripheral Neurotoxicity Test

For the PeriTox test, DoD8′ cells were thawed and seeded at a density of 0.1×10^6 cells per cm^2 in 50 μl of differentiation medium on Matrigel-coated 96-well dishes (BD Biosciences). Test chemicals were serially diluted in differentiation medium, and 50 μl was added to the cells, 1 hour after seeding. All analyses were performed 24 hours after treatment. The neurite area and viability were assessed as described in the supplemental online data. In brief, the cells were loaded with 1 μM calcein-AM and 1 μg/ml H-33342 for 1 hour at 37°C. For image acquisition, an ArrayScan VTI HCS (high-content imaging) microscope (Cellomics, Waltham, MA, http://thermofisher.com) was used. In an automated procedure, all $H\text{-}33342^+$/calcein-positive cells were analyzed as viable cells. The sum of fields evaluated for one data point contained 1,489 ± 485 healthy cells with a neurite area of 16,100 ± 4,000 pixels.

Quantitative Reverse-Transcription Real Time Polymerase Chain Reaction

RNA was extracted at the indicated DoD, and 1 μg of RNA was reversed transcribed (iScript, Bio-Rad Laboratories, Munich, Germany, http://www.bio-rad.com). For quantitative reverse-transcription real time polymerase chain reaction (qPCR), SsoFast EvaGreen Supermix was used on a Bio-Rad Light Cycler (Bio-Rad Laboratories). Real time quantification for each gene was normalized to the amount of RPL13A mRNA and expressed relative to the

transcript level in hESCs using the $2^{(-\Delta\Delta C(t))}$ method [28], as described in detail previously [29]. The list of primers is given in the supplemental online data.

Statistical Analysis

All experiments were repeated at least three times. Reference to replicates always means data from different cell preparations (thawings; i.e., biological replicates). Data are presented, using GraphPad Prism, version 5.0 (GraphPad Software, La Jolla, CA, http://www.graphpad.com), and statistical differences were tested by analysis of variance with post hoc tests as described in the supplemental online data.

RESULTS

Two-Step Differentiation of iDRG Cells From Pluripotent Stem Cells

To provide a sustainable supply of human peripheral neurons, we made use of a recently established protocol that allows conversion of hPSCs to differentiated sensory neurons [25]. A cryopreservation step was introduced on DoD8′ to allow the production of large cell lots, available after thawing as a population of rapidly differentiating neurons (Fig. 1, top). Immunostaining showed that the cells had different differentiation states on the day of freezing: a large (desired) subpopulation was $Sox10^+$ (neural crest marker, precursors of peripheral nervous system), few (undesired) cells were $PAX6^+$ (neuroepithelial marker for central nervous system precursors; Fig. 1A, left), and a few cells expressed $TUJ1^+$, an early neuronal marker (Fig. 1A, right). A more homogeneous population was obtained after thawing. Already at 8 hours after thawing, the developing cells were $TUJ1^+$ and had lost the precursor markers SOX10 (Fig. 1B) and PAX6 (data not shown). At 24 hours after thawing (DoD1), the neuronal marker TUJ1 indicated pronounced formation of early neurites (Fig. 1C). An upregulation of NeuN in $TUJ1^+$ cells indicated the generation of fully postmitotic neurons at DoD4 (Fig. 1D). Quantification of EdU incorporation showed that, already at DoD1, only a few proliferating cells (15%) were present; on DoD4, proliferation had virtually stopped (Fig. 1E). At DoD1, $TUJ1^+$ cells expressed BRN3A (Fig. 1F) and were positive for peripherin and ISL1 (Fig. 1G). At DoD4, these had formed a dense network. Strong and homogeneous expression of the transcription factor BRN3A (Fig. 1H) and positivity for peripherin and ISL1 (Fig. 1I) indicated that virtually all cells developed toward peripheral neurons.

A differentiation similar to the one of hESCs was also observed for a line of iPSCs (supplemental online Fig. 1A–1D). Our findings are in line with a recent characterization of a one-step protocol to generate sensory neurons [25, 30].

Functional Characterization of iDRG Cells

We investigated some functional properties of our iDRG cells at relatively early stages after thawing. First, the cellular response to depolarization was studied. Intracellular free calcium ($[Ca^{2+}]_i$) was measured after the addition of K^+ (50 mM) to the extracellular medium or after the opening of voltage-dependent Na^+-channels by veratridine. On DoD7, virtually all neuronal cells derived from hESCs or iPSCs showed a depolarization-induced increase of $[Ca^{2+}]_i$ (Fig. 2A; supplemental online Fig. 1E). The intracellular Ca^{2+} response was blocked by verapamil and nifedipine, inhibitors of voltage-dependent Ca^{2+} channels (Fig. 2B). Thus, the cells obtained by our 2-step protocol expressed functional veratridine-sensitive voltage-dependent Na channels and voltage-dependent Ca channels, as is typical for neurons and a few other excitable cells.

Differentiation Track of iDRG Cells

In order to provide a full characterization of cell identity at different stages (hESCs, DoD8′, DoD1, DoD4, and DoD7) of the 2-step differentiation procedure, we used transcriptome profiling. A principal component analysis (PCA) showed that replicates from four differentiations clustered closely together and that each differentiation state had clearly distinct characteristics (Fig. 3A). The large number of 5,000–8,800 probe sets were significantly altered when the differentiating cells were compared with hESCs (Fig. 3B). The regulated genes were assigned to different clusters according to the time course of their change: cluster I comprised genes continuously upregulated over time; cluster II contained genes that were upregulated during the first 8 days of differentiation and then stayed constant in their expression level; cluster III included the genes that were downregulated on differentiation (Fig. 3C). To put these changes into a defined general context, we generated a PCA "cell feature map" by plotting our data together with a large set of legacy data. As robust calibration points, we used CellNet (available at: http://cellnet.hms.harvard.edu/) [31] data from human liver (n = 252) and brain (n = 335). Moreover, we added data on primary human DRG, hESCs, various hPSC-derived cells [26, 27, 30], and fetal human neural precursors (LUHMES Lu0), sequentially differentiating (Lu3) to postmitotic central neurons in vitro (Lu6) [26, 32]. This novel approach of PCA mapping within a biological context showed that all in vitro neuro-differentiations caused a transcriptome shift from hESCs toward brain samples. Our two-step protocol and the older one-step protocol followed the same track (Fig. 3, red arrows) to get closer to human DRGs. The DoD4 of our two-step protocol (i.e., 13 days of differentiation from hESCs) was closer to DRGs than DoD16* of the one-step protocol. This suggests that the additional freezing and thawing step actually accelerated iDRG differentiation. The LUHMES differentiation pointed in the same direction but showed a clear separation from the iDRG differentiation (Fig. 3A). Having found this distinct and clear overall differentiation track of the iDRG cells, we examined functionally linked groups of genes. The gene ontology terms (GOs) that were most overrepresented among the genes upregulated on DoD1 were, for example, "neuron migration," "nervous system development," and "dendrite morphogenesis," and the most significant GOs were largely similar for iDRG cells and later stage neurons (DoD7). The top GOs overrepresented among the downregulated transcripts at DoD1 included "somatic stem cell maintenance" and "endodermal cell fate specification." The GO overrepresentation analysis therefore confirmed neurodifferentiation as a major biological process on the level of gene regulation, and this was paralleled by inhibition of non-neuronal lineage maintenance/differentiation (supplemental online Fig. 2A).

The top 20 individual transcripts upregulated at DoD1 included the neurogenic differentiation factors NeuroD1, SIX1,

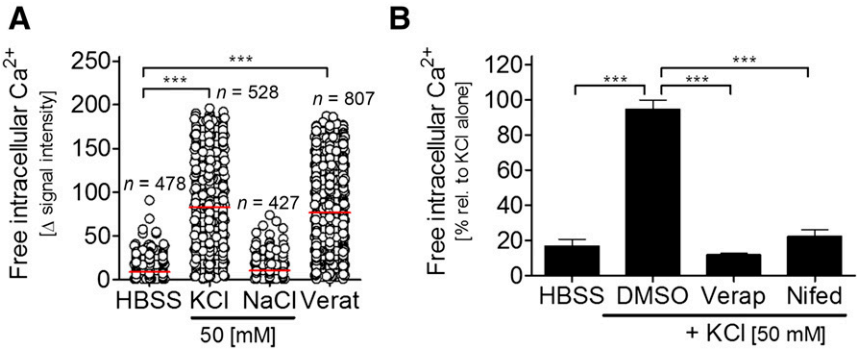

Figure 2. Quantification of calcium signaling of immature dorsal root ganglia neuron cells. **(A):** Intracellular calcium levels measured on DoD7 after depolarization. Each cell is depicted by a circle. ***, $p < .001$. **(B):** Before depolarization by KCl, cells were pretreated with Verap (100 μM) or Nifed (100 μM; $n = 3$; ***, $p < .001$). Abbreviations: DMSO, dimethyl sulfoxide; HBSS, Hanks' buffered salt solution; Nifed, nifedipine; rel., relative; Verap, verapamil; Verat, veratridine.

and EBF1, and the peripheral neuron subtype specifiers POU4 (BRN3A) and ISL1 (Fig. 3D; supplemental online Fig. 2B). Also when the transcriptome difference was measured between DoD8′ and DoD7, a significant overrepresentation of neuronal GO terms was still present among the upregulated genes (7 of the top 10), and 9 of the top 10 overrepresented GOs among the downregulated genes dealt with DNA replication and other DNA-related processes (supplemental online Fig. 2B, 2C). This is well in line with the results from a KEGG pathway overrepresentation analysis (supplemental online Fig. 2D) and with the phenotypically observed neuronal differentiation and the mitotic exit of the cells during that time period. The expression of a broad range of differentiation markers was confirmed by qPCR. Markers of sensory neurons (i.e., peripherin, ISL1, runt-related transcription factor 1 [RUNX1], vesicular glutamate transporter 2 [VGLUT 2], and the receptor tyrosine kinase RET) were upregulated. Also, the purinergic receptor P2RX3 and nociceptive markers such as TRPM8 or the sodium channels SCN9A and SCN10A were upregulated during differentiation (Fig. 3E).

Toxicant Sensitivity of Early Neurite Growth

In accordance with the neuronal gene expression pattern, the cells had already developed distinct neurites at DoD1 after thawing. The growth cones showed the characteristic distribution of microtubules (more toward the somata) and F-actin (at the tip) (Fig. 4A). In order to quantify neurite growth, the total neurite area was quantified at several time points after plating of the cells. The work flow we used was based on fully automated live cell microscopy, differential staining of nuclei and of the entire cytosol, followed by computational identification and quantification of the cellular parts (neurites) not belonging to the cell soma area (supplemental online Fig. 3A). The neurite area increased continuously from a few hours after plating until DoD4 (Fig. 4B).

In addition to the neurite area per imaging field, the imaging algorithm we used also yielded the number of viable cells by quantifying the ratio of cell bodies that were positive or negative for the viability dye calcein. This allowed us to investigate whether drug effects on neurite growth would occur independently of general cytotoxicity.

For a technical assessment of the test performance, we used rotenone (10 μM) as a positive control, because this compound has been shown in many other systems to affect neurites [16, 33–35]. Inhibition of neurite growth was quantified in 10 different cell preparations. The data suggested a sufficient signal-to-noise ratio of the test, as expressed by an average z′ factor of 0.7 (supplemental online Fig. 3B). To study concentration-dependent changes in detail, we used cytoskeletal toxicants as mechanism-focused positive controls. The microtubule toxicants vincristine and colchicine and the actin polymerization inhibitor cytochalasin D reduced neurite growth with high potency, without affecting general cell viability (Fig. 4C; supplemental online Fig. 1G–1I; supplemental online Fig. 3B, 3C). In summary, these data suggest that specific toxicant effects on neurites can be assessed in iDRG cells and be separated from general cytotoxicity.

In order to test at which state of neuronal developments the best test results were obtained, we performed toxicity testing of five compounds under standard conditions (i.e., in the 24-hour period following plating; no neurites present at the start of testing), and 3 days later, when an elaborate neurite network was already established. A comparison of the selectivity ratios (i.e., neurite toxicity versus general cytotoxicity) showed that the use of immature neurons (DoD1) provided clearly superior test performance (supplemental online Fig. 3D). This condition was therefore chosen as the standard setup for a human neurite-based PeriTox test.

Basic Characterization of the PeriTox Test

Two types of negative controls were tested. The first subgroup comprised compounds not (<20% of control) assumed to affect any test endpoint. Acetylsalicylic acid (data not shown) and mannitol (Fig. 5A) showed such behavior at concentrations up to the mM range. The second subgroup comprised compounds that affected viability and neurites in the same concentration range (unspecific controls). The detergents sodium dodecyl sulfate (SDS) and Triton X-100 showed this behavior, as expected (Fig. 5B). As a signaling pathway-specific control for PeriTox test performance, we used the guanylyl cyclase inhibitor ODQ, which is known to disrupt human neurite growth [36]. This drug was confirmed to affect neurites without other cellular toxicity (Fig. 5C; supplemental online Fig. 1I). It was therefore used as an acceptability control for further test runs (neurite reduction >40%). To test more stringently

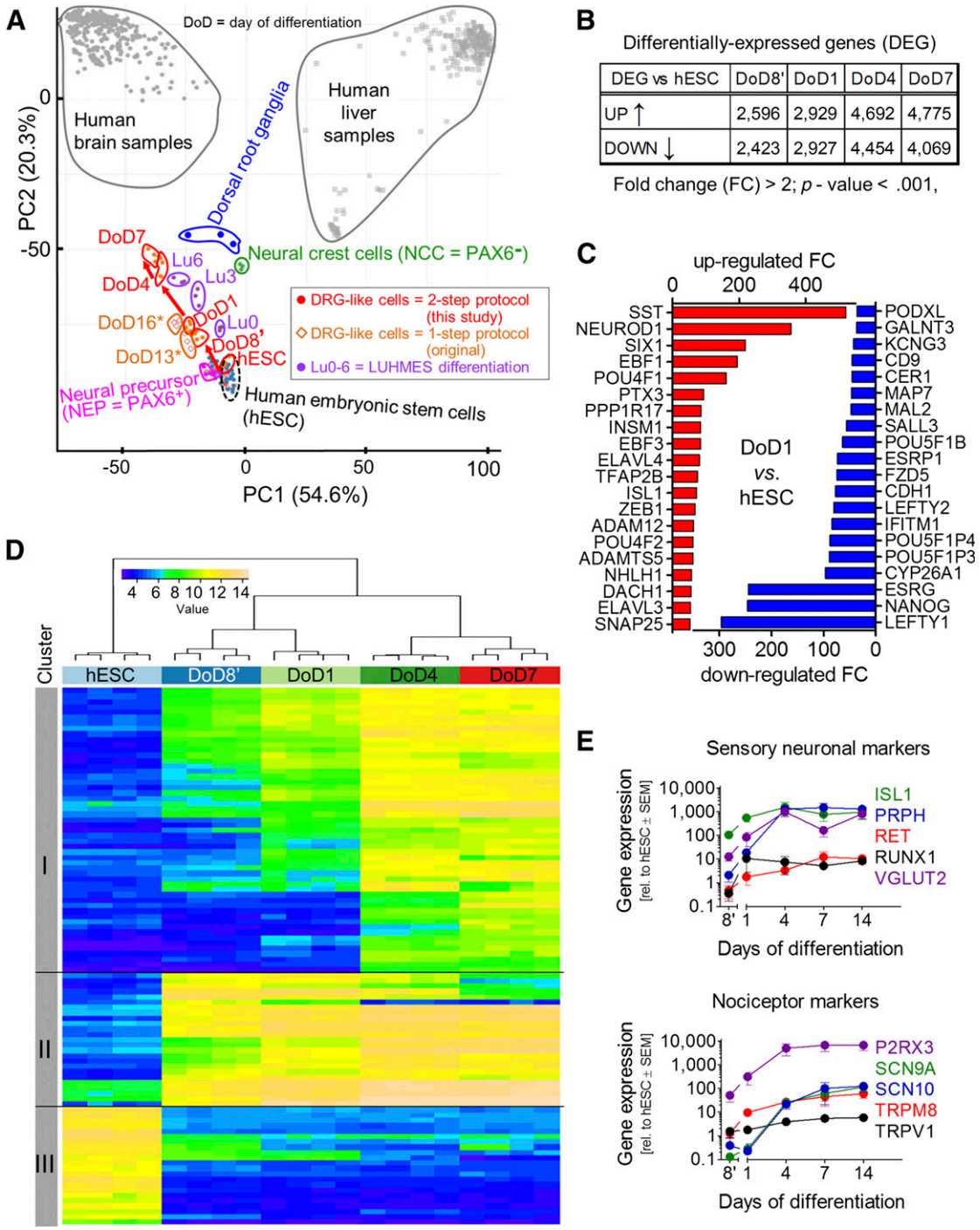

Figure 3. Differentiation tracking by transcriptome analysis of iDRG cells. **(A):** Samples were obtained at different developmental stages for whole transcriptome analysis; data are displayed as a principal component analysis (PCA) map, together with legacy data from cell cultures or from human dorsal root ganglion, brain, and liver tissue. The red arrow indicates the cell differentiation track of the two-step iDRG cell differentiation protocol. Note: DoD7 of the two-step protocol is 16 days older than hESCs (i.e., roughly corresponding to DoD16* of the one-step protocol in differentiation time). **(B):** Number of regulated genes over time. **(C):** Top 20 significantly upregulated (red) and downregulated (blue) genes. **(D):** Hierarchical clustering analysis of the top 100 genes with the highest variance during peripheral neuronal differentiation. **(E):** Relative gene expression during differentiation (n = 4–6). Abbreviations: DoD, day of differentiation; FC, fold change; hESC, human embryonic stem cell; iDRG, immature dorsal root ganglia neuron; PC1, principal component 1; PC2, principal component 2; rel., relative.

whether the neurite effects detected in the PeriTox test could be fully uncoupled from cytotoxicity, we performed drug washout/recovery experiments. The standard test was run with 200 μM ODQ (for 24 hours). Then, the drug was washed out, and we observed complete recovery (i.e., regrowth of the neurites up to the level of untreated controls; Fig. 5D). The ROCK inhibitor Y-27632 was used as a second pathway-specific control (for accelerated growth pathways) to explore

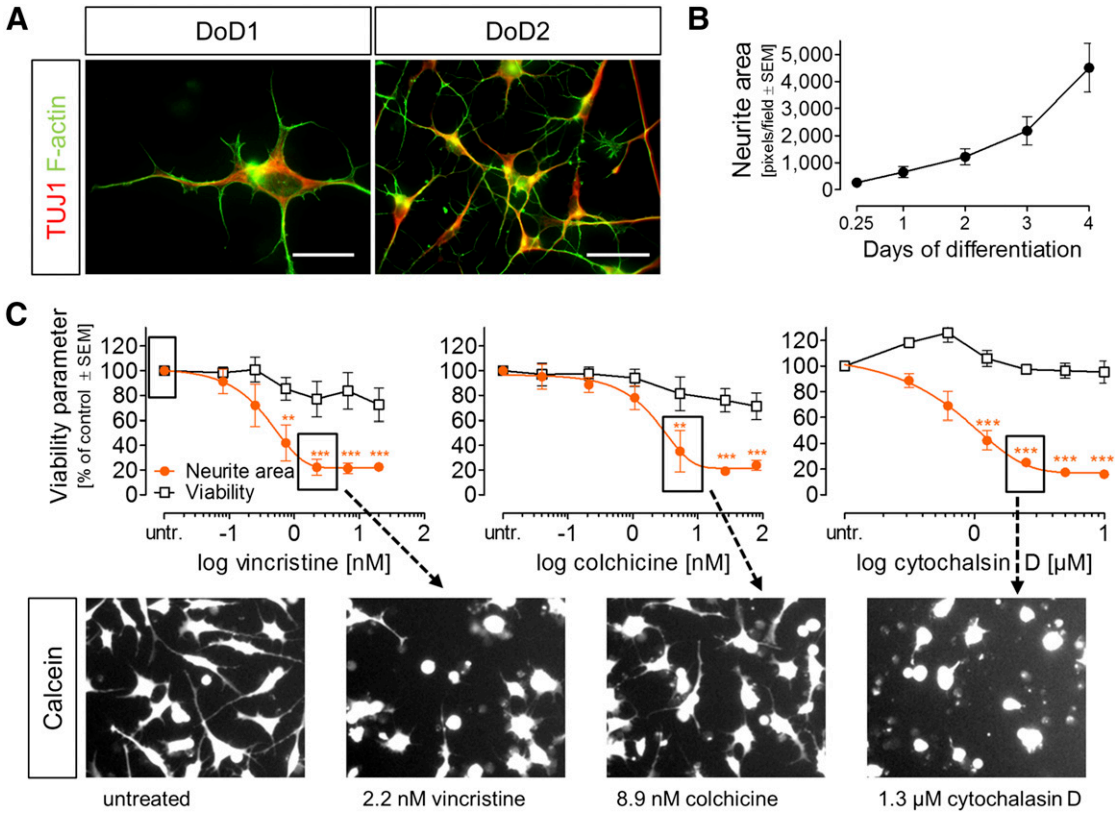

Figure 4. Characterization and quantification of neurite growth of early iDRG cells. **(A):** Immunocytochemical characterization of early neurites; labels are color keyed to images. **(B):** Quantification of neurite area over time (mean ± SEM; $n = 5$). **(C):** Effects of vincristine, colchicine, and cytochalasin D on neurite area and viability under PeriTox test conditions (mean ± SEM; $n = 3$–4) and exemplary sample images (**, $p < .01$; ***, $p < .001$). Scale bars = 20 μm **(A, left)** and 50 μm **(B, right; C)**. Abbreviations: DoD, day of differentiation; untr., untreated.

the dynamic range of the assay. The PeriTox test data suggested that growth-accelerating compounds can also be detected (Fig. 5E).

After these basic assay controls, we explored the sensitivity for clinically used drugs known to cause peripheral neuropathies in humans [1, 2, 37–39]. Cisplatin and bortezomib significantly affected the neurites at concentrations showing no effect on viability (Fig. 5F). Thus, the PeriTox test fulfilled all the basic requirements of a cellular toxicological assay.

Toxicant Screening and Set Up of a PeriTox Test Prediction Model

To design a prediction model for the PeriTox test, we took the following steps: (a) use of the "ratio" of EC_{50} (viability)/EC_{50} (neurites) as the primary endpoint; (b) measurement of this value for "unspecific toxicants" (the uncoupler CCCP, SDS, Triton-X100, and the topoisomerase inhibitor etoposide; the average ratio was 1.37 ± 0.39); (c) definition of a "noise band" (4 SD from the average of the ratios of these compounds); and (d) definition of compounds with a ratio outside the noise band (EC_{50} ratio of >3) as "neurite specific."

This test definition was used to screen three dozen chemicals, preselected for their potential interest for neurite toxicity. Altogether, 21 positive hits were identified. All microtubule drugs and proteasome inhibitors were classified as positive hits. This also included the new drug class of epothilones [40, 41], which we found to damage neurites without affecting cell viability (supplemental online Fig. 3E, 3F). All these data were in good agreement with recent clinical findings. Several histone deacetylase (HDAC) inhibitors (HDACi; MS275, SAHA, and TSA) showed neurite toxicity. Among the ROCK pathway modulators, the ρ activator narciclasine was toxic to neurites (Fig. 6A, 6B) and inhibitors, such as blebbistatin, accelerated neurite growth (not shown).

Application of PeriTox Test to Environmental Toxicants

Neurotoxicity testing of environmental chemicals is particularly challenging, as their effects on neurites in vivo often requires prolonged exposure. The final toxicity outcome might result from continuous damage accumulation, a process difficult to reproduce in vitro. Therefore, we explored the hypothesis that the particular requirements of neurites that are still growing will "sensitize" the cells to neurotoxicants [16] and that this would allow detection of toxicity in the PeriTox test, although it is a short-term assay. We found that 24 hours of exposure to acrylamide significantly reduced the neurite area at concentrations of ≥875 μM but that viability was reduced only at higher (≥4.7 mM; EC_{50} ratio of 3.2) concentrations (Fig. 7A). A comparison of the toxicant sensitivity of growing neurites (DoD1) with that of established neurites (DoD4) showed that selective neurite damage was more readily observed in the neuronal cultures with growing neurites (supplemental online Fig. 3D). The structurally related negative control acrylic acid showed hardly any effect on neurites or viability (Fig. 7B). Immunostaining for

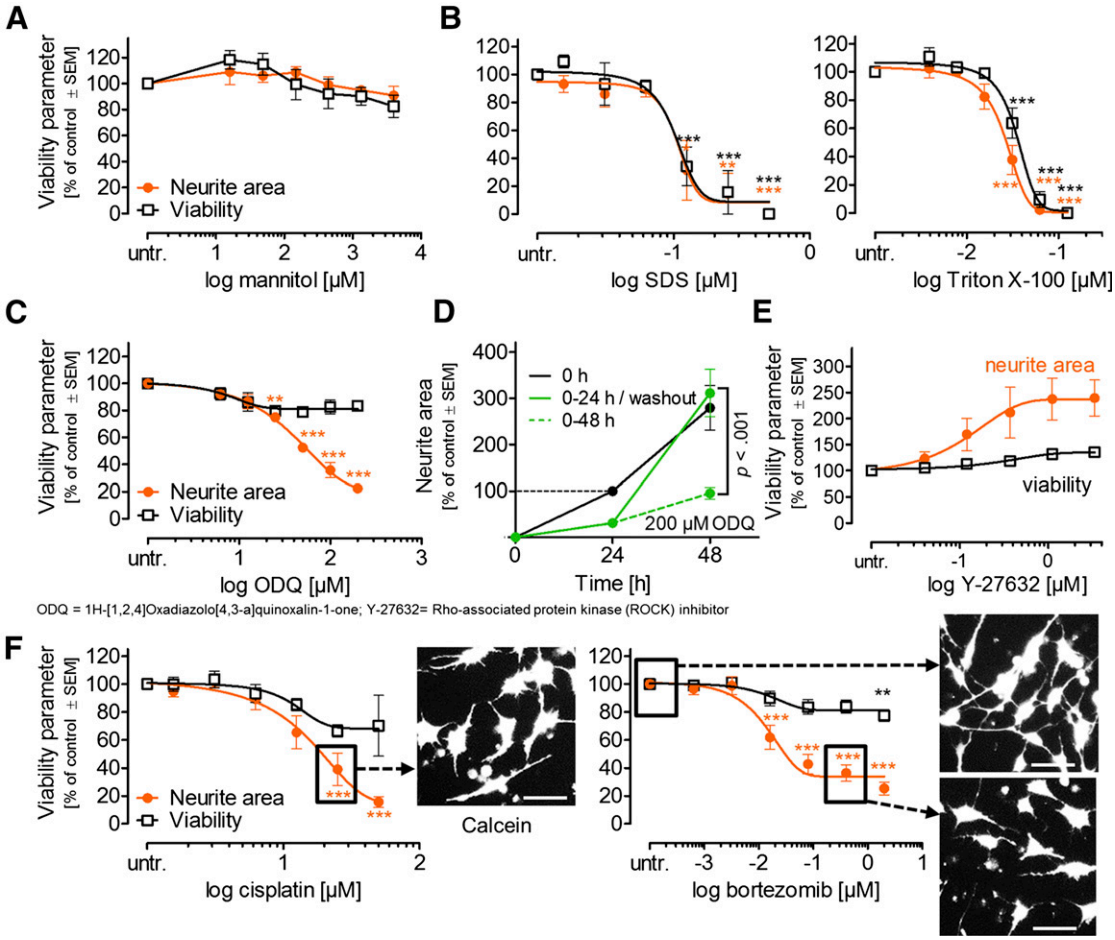

Figure 5. Profiling and quantification of negative and positive control toxicant effects on immature dorsal root ganglia neuron neurites. Tool compounds were used as in **(4C)**. **(A):** Negative control. **(B):** Unspecific toxicants. **(C):** Guanylyl cyclase inhibitor as pathway-specific control. *, $p < .05$; **, $p < .01$; ***, $p < .001$ versus untr. cells. **(D):** Test of reversibility. After 24 hours of exposure, ODQ was washed out, and neurites were measured again 24 hours later ($n = 3–4$). **(E):** ROCK inhibitor as pathway-specific control for accelerated growth. **(F):** Positive controls (drugs causing peripheral neuropathy). Scale bars = 50 μm. Abbreviations: SDS, sodium dodecyl sulfate; untr., untreated.

the microtubule marker TUJ1 showed that acrylamide-treated cells still had elaborate cytoskeletal structures but shortened neurites (Fig. 7C). Moreover, the partial reversibility of the acrylamide-induced effect on neurites suggests that the cells remained viable in the presence of the drug: after a washout, the neurons significantly accelerated their neurite growth compared with cells that continued to be treated with the chemical (Fig. 7D).

Arsenic is another environmental toxicant known to induce neuropathies. Exposure to sodium arsenate resulted in an EC_{50} ratio (viability/neurites) of >7. This large offset led to its classification as a neurotoxicant in the PeriTox test (Fig. 7E). For the related compound, arsenic trioxide, some concentrations (0.6–2.5 μM) significantly affected the neurites without cytotoxicity. As the EC_{50} ratio was only 2.3, this chemical would not be classified as a neurite toxicant (Fig. 7F). Finally, the pesticide rotenone was clearly predicted as a neurite toxicant by our prediction model (EC_{50} ratio >50; Fig. 7G). A recovery experiment showed that cells started growing neurites again after rotenone (0.4–2 μM) washout and had nearly completely caught up with untreated controls by 24 hours after washout (Fig. 7H).

PeriTox Test Performance Versus Established LUHMES Neurite Assay

To obtain data on test specificity, we first compared the results of the PeriTox test with published data from the LUHMES neurite test [16]. Several compounds with diverse modes of actions behaved similarly in the two assays. However, acrylamide, bortezomib, cisplatin, and Taxol, all known for causing human peripheral neuropathies, were only detected by the PeriTox test (Fig. 6B). Thus, our new method made full use of the potential of human stem cell technology to identify a large number of human-relevant peripheral neurotoxicants not identified by the LUHMES assay (supplemental online Fig. 4). Therefore, we consider it an important addition to the battery of existing in vitro tests able to alert for potential neurotoxic hazard of drugs and environmental chemicals.

Discussion

Despite the large incidence of peripheral neuropathies (PNs), a dearth of studies is available on relevant human cells. Diabetic PNs has reached a two-digit incidence in the U.S. population

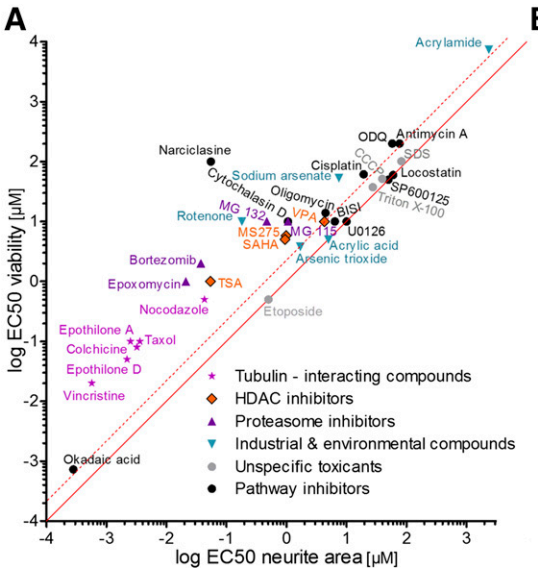

EC50 ratio	PeriTox	LUHMES
Acrylamide	3.2	2.4
Bortezomib	54	1
Cisplatin	3.2	1.4
Cytochalasin D	9.4	2
MG 132	21	1
Oligomycin	3.1	1.8
TSA	19	1
Y-27632	> 100	9.4
Colchicine	25	> 100
Epothilone	40	25
Narciclasine	> 100	> 100
Nocodazole	12	> 100
ODQ	3.5	3.9
Rotenone	56	> 100
Vincristine	35	> 100
U0126	1	16
BIS I	1.6	8.3

Figure 6. Classification of toxicant effect on immature dorsal root ganglia neuron neurites. **(A):** Overview of specificity of all compounds tested. EC_{50} values for effects on neurite area were plotted against EC_{50} for effects on viability. The solid line indicates an EC_{50} ratio of 1. The dashed line indicates an EC_{50} ratio of 3 ($n \geq 3$). **(B):** Comparison of positive hits in the PeriTox test and published data on the LUHMES test (based on central neurons). For both tests, the EC_{50} ratio (EC_{50} viability to EC_{50} neurite area) of various compounds is shown. Abbreviation: HDAC, histone deacetylase.

[42]. Also, >60% of chemotherapy patients develop PNs [43], and several other drug classes [44] have been associated with PNs. Moreover, several environmental chemicals either trigger PN or can affect neurites during development [17]. For example, acrylamide causes axonal degeneration of exposed workers by affecting the microtubules of the neurites without causing cell death [2]. Moreover, most chemotherapeutic agents are known to induce specific axonal neuropathies [1, 38]. As a method to evaluate such toxicity on human peripheral neurons has not been available, the PeriTox test represents pivotal progress toward filling this gap.

The first important step was the optimization of a protocol that allowed the generation of iDRG cells at the amounts and with the quality and reproducibility required for a quantitative toxicological assay. The second pivotal step was the identification and use of a functional endpoint that allowed sufficient throughput, unbiased quantification, and development of a prediction model to distinguish specific neurite toxicity from general cytotoxicity. The PeriTox test reacted correctly (sensitivity of 87%) to many known human PN toxicants, and it discriminated (specificity of 100%) between peripheral neurotoxicants and chemicals not expected to cause PN.

The successful establishment and evaluation of the PeriTox test builds on a test development research line that has become increasingly more important in the field: transition from rodent primary cells or from transformed human cells to nontransformed human stem cell-derived specialized cells with characteristics of the relevant target tissue. In the past, rodent sensory neurons/DRG have allowed important studies of the mechanisms of peripheral neurotoxicity/degeneration [45, 46]. However, the overwhelming majority of reports in this area focused on the underlying mechanisms and never compared more than three toxicants. Although stem cell technology has paved the way toward the use of human nontransformed cells, past assays have been built on central neurons and never worked for more than three specific toxicants [18, 47]. The LUHMES system (using conditionally immortalized central neuronal precursor cells) was the first assay in the field identifying >20 toxicants and systematically examining the relation of neurite growth, neurite toxicity, and cytotoxicity [16]. However, LUHMES are central neurons and derived from conditionally immortalized cells. It was assumed that the most relevant target cell type (i.e., peripheral neurons to test for peripheral neurotoxicity) would produce the most reliable results, because many examples of cell type-dependent toxicity are available. For instance, the chemotherapeutic drug cisplatin accumulates faster in primary sensory neurons than in PC12 cells [39], the toxicant effects on neural crest cell migration differs from effects of the same chemical on neural precursor cells or tumor cells [27], and even the subtypes of dopaminergic neurons showed different sensitivity in their vulnerability to the toxicant MPTP [48]. The PeriTox test has taken a large step past the LUHMES assay by using nonengineered iDRG cells that detected several known PN toxicants missed by the LUHMES assay.

That we observed reversibility of some toxicant action (e.g., rotenone) might be important for future applications in risk assessment. Moreover, this feature will allow screens for recovery-enhancing compounds, and the use of a panel of iPSCs for the PeriTox test would even consider individual genetic determinants of toxicity/recovery [47].

The test results from a mixed group of toxicants used in the present study showed that not only were well-known hazardous drugs and environmental compounds identified, but also potentially neuroprotective drugs (ROCK inhibitors) and so-called alerts (HDACi) were marked for further follow-up. We gave the thorough characterization of the developmental stage of the neurons particular attention. On the one hand, the PeriTox test was designed as a neurotoxicity assay that makes use of the fact that growing neurites of cultured cells are particularly

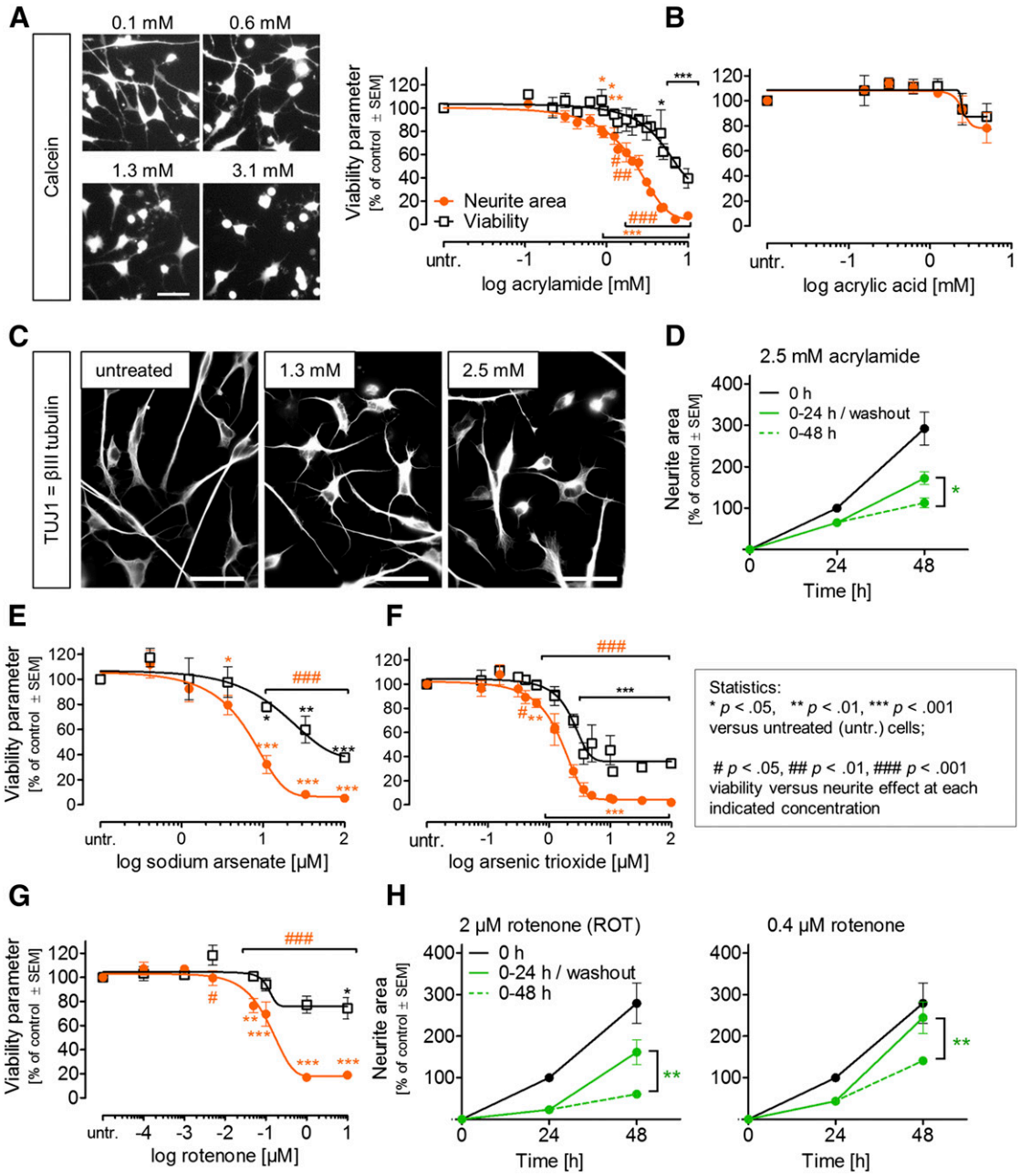

Figure 7. Effect of environmental toxicants on immature dorsal root ganglia neuron neurites. Neurite area and viability were measured under PeriTox test conditions. Effect of acrylamide **(A)** or acrylic acid **(B)** (mean ± SEM; $n = 3–5$). **(C):** Immunostaining of cells treated with acrylamide as in **(A)**. **(D):** Test of reversibility. After 24 hours of exposure, acrylamide was washed out, and neurites were measured again 24 hours later ($n = 3–4$). **(E–G):** Toxicant testing as in **(A)**. **(H):** Reversibility of rotenone effects was tested as in D. Scale bars = 50 μm **(A, C)**.

sensitive to neurotoxicants. This approach allowed us to overcome the largest problem of in vitro assays in this field [16] (i.e., the separation of specific neurite effects from unspecific cell death). On the other hand, an added benefit could also be that some developmental toxicants could be identified [8, 49]. This might be why the PeriTox test produced an alert on the emerging class of HDACi-based chemotherapeutic agents (and known developmental toxicants) as potential peripheral neurotoxicants. Additional patient observations are required to decide whether such predictions hold true in clinical situations (supplemental online Fig. 4).

Conclusion

The generation of immature dorsal root ganglia neurons from human pluripotent stem cells provided the basis for a drug and chemical safety evaluation assay on cells not otherwise available. Testing of more than 30 chemicals showed that human neurotoxicants and neurite growth enhancers were correctly identified. The adaptations of the protocols we have described (e.g., the introduction of a freeze-thaw step and the strong focus on the initial neurite growth phase) resulted in an assay that is specific for neurotoxicants (in contrast to cytotoxicants) and is very robust across different operators and assay

runs. Various classes of chemotherapeutic agents causing human peripheral neuropathies were identified, although they were missed when tested on human central neurons. The PeriTox test we established shows the potential of human stem cells for clinically relevant safety testing of drugs in use and new emerging candidates.

Acknowledgments

This work was supported by national Doerenkamp-Zbinden Foundation, Konstanz Graduate School Chemical Biology KORS-CB, Research Training Group 1331 (RTG), and BMBF (German Ministry of Education and Research) grants. We thank Alex Gutteridge (Pfizer) for providing primary dorsal root ganglia neuron transcriptome data. Technical assistance from M. Kapitza and advice from B. Zimmer are gratefully acknowledged.

Author Contributions

L.H.: conception and design, collection and assembly of data, data analysis and interpretation, manuscript writing, final approval of manuscript; S.K., M.G., J.M., J.R., and N.B.: collection and assembly of data, data analysis and interpretation; C.K.: data analysis and interpretation; M.H., T.R., and A.S.: collection and assembly of data; T.W.: conception and design, data analysis and interpretation; M.L.: conception and design, data analysis and interpretation, manuscript writing, final approval of manuscript.

Disclosure of Potential Conflicts of Interest

M.L. is a compensated consultant for the European Food Safety Authority and the Doerenkamp-Zbinden Foundation, has received compensated honoraria and uncompensated research funding from the Doerenkamp-Zbinden Foundation and the Center for Alternatives to Animal Testing-Europe, and has provided uncompensated expert testimony for the Swiss Centre for Applied Human Toxicology. The other authors indicated no potential conflicts of interest.

References

1 LoPachin RM, Gavin T. Toxic neuropathies: Mechanistic insights based on a chemical perspective. Neurosci Lett 2014; 596:78–83.

2 Spencer PS, Schaumburg HH. Experimental and Clinical Neurotoxicology. New York: Oxford University Press, 2000.

3 Kuegler PB, Zimmer B, Waldmann T et al. Markers of murine embryonic and neural stem cells, neurons and astrocytes: Reference points for developmental neurotoxicity testing. ALTEX 2010;27:17–42.

4 Knudsen TB, Keller DA, Sander M et al. FutureTox II: In vitro data and in silico models for predictive toxicology. Toxicol Sci 2015;143: 256–267.

5 Bouvier d'Yvoire M, Bremer S, Casati S et al. ECVAM and new technologies for toxicity testing. Adv Exp Med Biol 2012;745:154–180.

6 Kolaja K. Stem cells and stem cell-derived tissues and their use in safety assessment. J Biol Chem 2014;289:4555–4561.

7 Hartung T, Leist M. Food for thought ... on the evolution of toxicology and the phasing out of animal testing. ALTEX 2008;25:91–102.

8 Bal-Price A, Crofton KM, Leist M et al. International STakeholder NETwork (ISTNET): Creating a developmental neurotoxicity (DNT) testing road map for regulatory purposes. Arch Toxicol 2015;89:269–287.

9 Tice RR, Austin CP, Kavlock RJ et al. Improving the human hazard characterization of chemicals: A Tox21 update. Environ Health Perspect 2013;121:756–765.

10 Collins FS, Gray GM, Bucher JR. Toxicology: Transforming environmental health protection. Science 2008;319:906–907.

11 Radio NM, Freudenrich TM, Robinette BL et al. Comparison of PC12 and cerebellar granule cell cultures for evaluating neurite outgrowth using high content analysis. Neurotoxicol Teratol 2010;32:25–35.

12 Howard AS, Bucelli R, Jett DA et al. Chlorpyrifos exerts opposing effects on axonal and dendritic growth in primary neuronal cultures. Toxicol Appl Pharmacol 2005;207:112–124.

13 Kim WY, Gonsiorek EA, Barnhart C et al. Statins decrease dendritic arborization in rat sympathetic neurons by blocking RhoA activation. J Neurochem 2009;108: 1057–1071.

14 Frimat JP, Sisnaiske J, Subbiah S et al. The network formation assay: A spatially standardized neurite outgrowth analytical display for neurotoxicity screening. Lab Chip 2010;10: 701–709.

15 Valdivia P, Martin M, LeFew WR et al. Multi-well microelectrode array recordings detect neuroactivity of ToxCast compounds. Neurotoxicology 2014;44:204–217.

16 Krug AK, Balmer NV, Matt F et al. Evaluation of a human neurite growth assay as specific screen for developmental neurotoxicants. Arch Toxicol 2013;87:2215–2231.

17 Stiegler NV, Krug AK, Matt F et al. Assessment of chemical-induced impairment of human neurite outgrowth by multiparametric live cell imaging in high-density cultures. Toxicol Sci 2011;121:73–87.

18 Harrill JA, Freudenrich TM, Machacek DW et al. Quantitative assessment of neurite outgrowth in human embryonic stem cell-derived hN2 cells using automated high-content image analysis. Neurotoxicology 2010;31: 277–290.

19 Oyebode OR, Hartley R, Singhota J et al. Differential protection of neuromuscular sensory and motor axons and their endings in Wld(S) mutant mice. Neuroscience 2012;200: 142–158.

20 Gilley J, Orsomando G, Nascimento-Ferreira I et al. Absence of SARM1 rescues development and survival of NMNAT2-deficient axons. Cell Reports 2015;10:1974–1981.

21 Di Stefano G, Manerba M, Vettraino M. NAD metabolism and functions: A common therapeutic target for neoplastic, metabolic and neurodegenerative diseases. Curr Top Med Chem 2013;13:2918–2929.

22 Kadereit S, Zimmer B, van Thriel C et al. Compound selection for in vitro modeling of developmental neurotoxicity. Front Biosci (Landmark Ed) 2012;17:2442–2460.

23 Crofton KM, Mundy WR, Shafer TJ. Developmental neurotoxicity testing: A path forward. Congenit Anom (Kyoto) 2012;52: 140–146.

24 Thomson JA, Itskovitz-Eldor J, Shapiro SS et al. Embryonic stem cell lines derived from human blastocysts. Science 1998;282:1145–1147.

25 Chambers SM, Qi Y, Mica Y et al. Combined small-molecule inhibition accelerates developmental timing and converts human pluripotent stem cells into nociceptors. Nat Biotechnol 2012;30:715–720.

26 Krug AK, Kolde R, Gaspar JA et al. Human embryonic stem cell-derived test systems for developmental neurotoxicity: A transcriptomics approach. Arch Toxicol 2013;87:123–143.

27 Zimmer B, Lee G, Balmer NV et al. Evaluation of developmental toxicants and signaling pathways in a functional test based on the migration of human neural crest cells. Environ Health Perspect 2012;120:1116–1122.

28 Livak KJ, Schmittgen TD. Analysis of relative gene expression data using real-time quantitative PCR and the 2(-Delta Delta C(T)) method. Methods 2001;25:402–408.

29 Balmer NV, Weng MK, Zimmer B et al. Epigenetic changes and disturbed neural development in a human embryonic stem cell-based model relating to the fetal valproate syndrome. Hum Mol Genet 2012;21:4104–4114.

30 Young GT, Gutteridge A, Fox HD et al. Characterizing human stem cell-derived sensory neurons at the single-cell level reveals their ion channel expression and utility in pain research. Mol Ther 2014;22:1530–1543.

31 Cahan P, Li H, Morris SA et al. CellNet: Network biology applied to stem cell engineering. Cell 2014;158:903–915.

32 Scholz D, Pöltl D, Genewsky A et al. Rapid, complete and large-scale generation of post-mitotic neurons from the human LUHMES cell line. J Neurochem 2011;119:957–971.

33 Borland MK, Trimmer PA, Rubinstein JD et al. Chronic, low-dose rotenone reproduces Lewy neurites found in early stages of Parkinson's disease, reduces mitochondrial movement and slowly kills differentiated SH-SY5Y neural cells. Mol Neurodegener 2008;3:21.

34 Persson AK, Kim I, Zhao P et al. Sodium channels contribute to degeneration of dorsal root ganglion neurites induced by mitochondrial dysfunction in an in vitro model of axonal injury. J Neurosci 2013;33:19250–19261.

35 Sanchez M, Gastaldi L, Remedi M et al. Rotenone-induced toxicity is mediated by Rho-GTPases in hippocampal neurons. Toxicol Sci 2008;104:352–361.

36 Lee HG, Kim SY, Kim S et al. 1H-[1,2,4] oxadiazolo[4,3-a]quinoxalin-1-one inhibits neurite outgrowth and causes neurite retraction in PC12 cells independently of soluble guanylyl cyclase. J Neurosci Res 2009;87: 269–277.

37 Argyriou AA, Iconomou G, Kalofonos HP. Bortezomib-induced peripheral neuropathy in multiple myeloma: A comprehensive review of the literature. Blood 2008;112: 1593–1599.

38 Miltenburg NC, Boogerd W. Chemotherapy-induced neuropathy: A comprehensive survey. Cancer Treat Rev 2014;40:872–882.

39 McDonald ES, Randon KR, Knight A et al. Cisplatin preferentially binds to DNA in dorsal root ganglion neurons in vitro and in vivo: A potential mechanism for neurotoxicity. Neurobiol Dis 2005;18:305–313.

40 Argyriou AA, Marmiroli P, Cavaletti G et al. Epothilone-induced peripheral neuropathy: A review of current knowledge. J Pain Symptom Manage 2011;42:931–940.

41 Cardoso F, de Azambuja E, Lago LD. Current perspectives of epothilones in breast cancer. Eur J Cancer 2008;44:341–352.

42 Davies M, Brophy S, Williams R et al. The prevalence, severity, and impact of painful diabetic peripheral neuropathy in type 2 diabetes. Diabetes Care 2006;29:1518–1522.

43 Seretny M, Currie GL, Sena ES et al. Incidence, prevalence, and predictors of chemotherapy-induced peripheral neuropathy: A systematic review and meta-analysis. Pain 2014; 155:2461–2470.

44 Höke A, Ray M. Rodent models of chemotherapy-induced peripheral neuropathy. ILAR J 2014;54:273–281.

45 Staff NP, Podratz JL, Grassner L et al. Bortezomib alters microtubule polymerization and axonal transport in rat dorsal root ganglion neurons. Neurotoxicology 2013;39:124–131.

46 Gerdts J, Summers DW, Sasaki Y et al. Sarm1-mediated axon degeneration requires both SAM and TIR interactions. J Neurosci 2013;33:13569–13580.

47 Wheeler HE, Wing C, Delaney SM et al. Modeling chemotherapeutic neurotoxicity with human induced pluripotent stem cell-derived neuronal cells. PLoS One 2015;10: e0118020.

48 Chung CY, Seo H, Sonntag KC et al. Cell type-specific gene expression of midbrain dopaminergic neurons reveals molecules involved in their vulnerability and protection. Hum Mol Genet 2005;14:1709–1725.

49 Bal-Price A, Crofton KM, Sachana M et al. Putative adverse outcome pathways relevant to neurotoxicity. Crit Rev Toxicol 2015;45:83–91.

See www.StemCellsTM.com for supporting information available online.

